

T_{CMB} vs redshift and the Hubble diagram from the Sunyaev-Zel'dovich effect with Planck

Gemma Luzzi

Group Planck

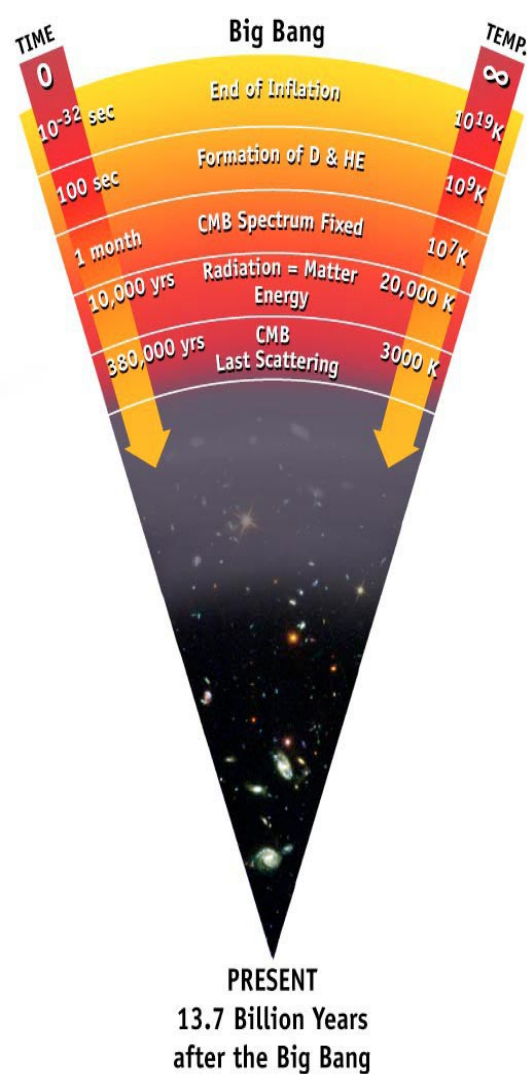
LAL Orsay

IAS Orsay, 3 February 2011

Outline

- CMB
- SZE
- $T_{\text{CMB}}(z)$
- Cluster parameter recovery with Planck HFI:
forecasts for H_0 and $T_{\text{CMB}}(z)$

Cosmic Microwave Background (CMB)



The Big Bang theory (Gamov 1948) foresees a primordial Universe which expands while cooling down.

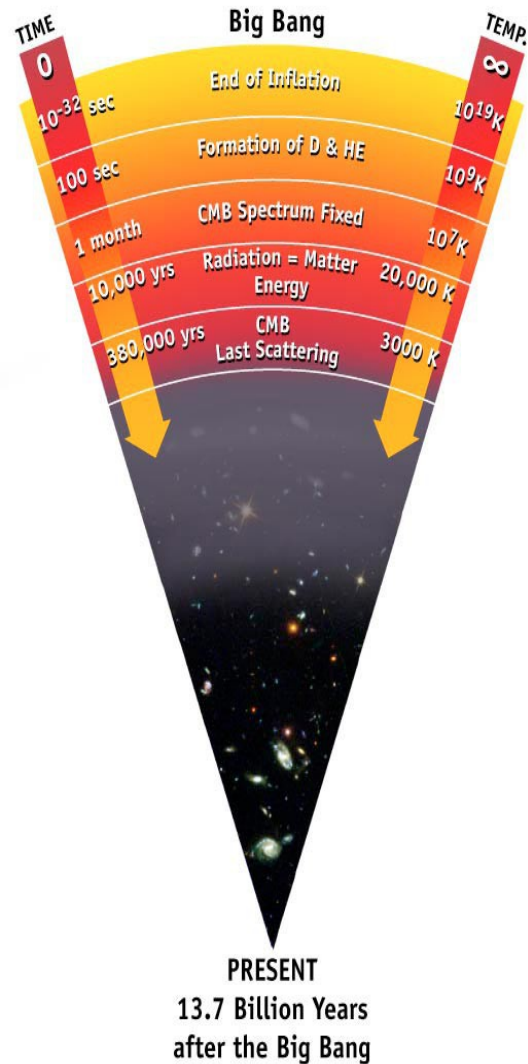
The early Universe can be described as a plasma, in which ionized matter is coupled to radiation through Thomson scattering.

When the temperature falls below 3000K (at $z \sim 1000$) electrons and protons recombine forming neutral hydrogen. Thomson scattering is no longer effective, therefore matter and radiation decouple.

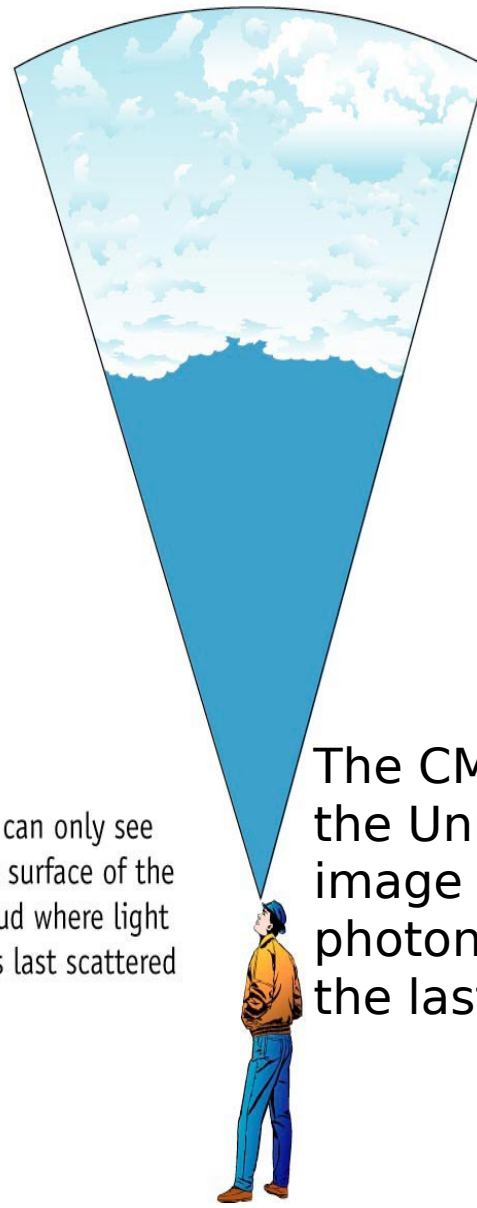
The mean free path of photons becomes larger than the causal horizon: photons can travel freely to us.

The cosmic microwave background Radiation's "surface of last scatter" is analogous to the light coming through the clouds to our eye on a cloudy day.

Cosmic Microwave Background (CMB)



The cosmic microwave background Radiation's "surface of last scatter" is analogous to the light coming through the clouds to our eye on a cloudy day.



We can only see the surface of the cloud where light was last scattered

The CMB is the dominant radiation field in the Universe.

Discovered in 1965 by Penzias and Wilson. One of the most powerful pieces of informations in support of Big Bang theory.

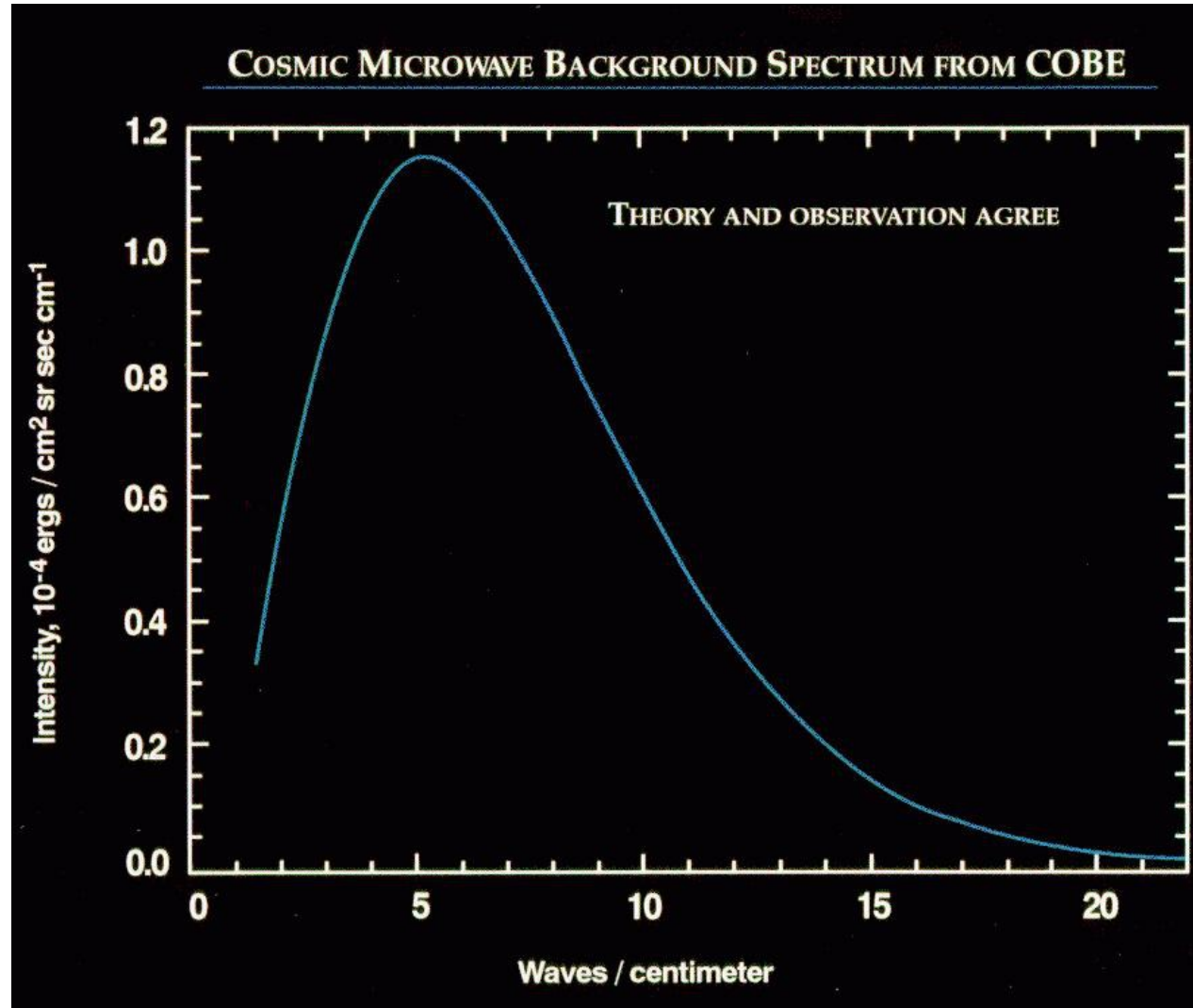
The CMB is interpreted as an image of the Universe at decoupling, that is the image of the surface from which photons were scattered by electrons for the last time.

CMB: BB spectrum

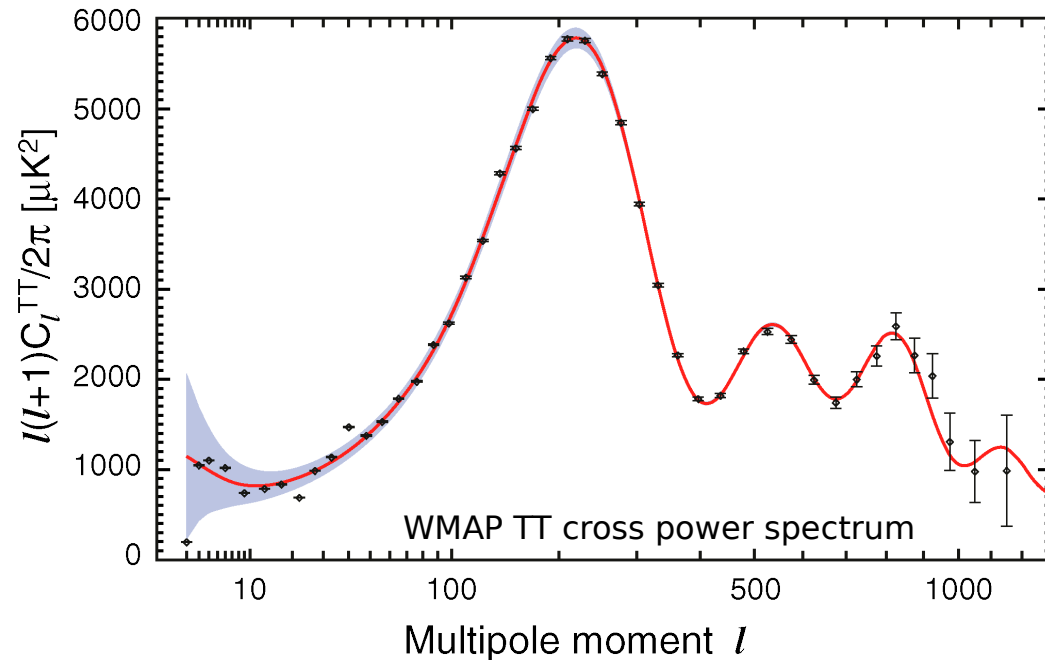
Being the CMB generated in a thermal equilibrium state, we expect a blackbody spectrum.

Observations by FIRAS on board COBE satellite have confirmed that the radiation is extremely close to the black body form at a temperature

$$T_0 = (2.725 \pm 0.002) \text{K}$$



CMB: power spectrum



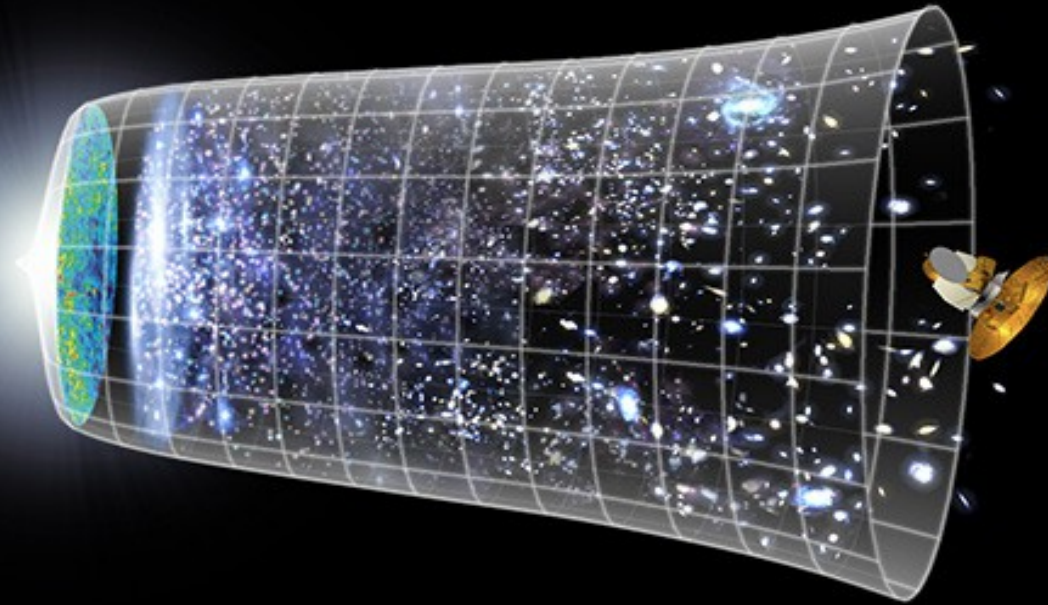
The inhomogeneities in the matter distribution at $z=1000$ produced intensity fluctuations of the radiation field:

Primary Anisotropies

Predicted anisotropies are very sensitive to a wide range of cosmological parameters: accurate measurements of them provide excellent constraints on cosmological models.

Secondary anisotropies from galaxy clusters

There are a number of structures in the Universe that can affect the propagation of radiation between the decoupling epoch and the present, which lead to **secondary anisotropies**.



Clusters of galaxies, which are the most massive well differentiated structures in the Universe, introduce secondary anisotropies: both metric perturbations (**Rees-Sciama**) and due to comptonization of the CMB (**Sunyaev Zel'dovich effect**).

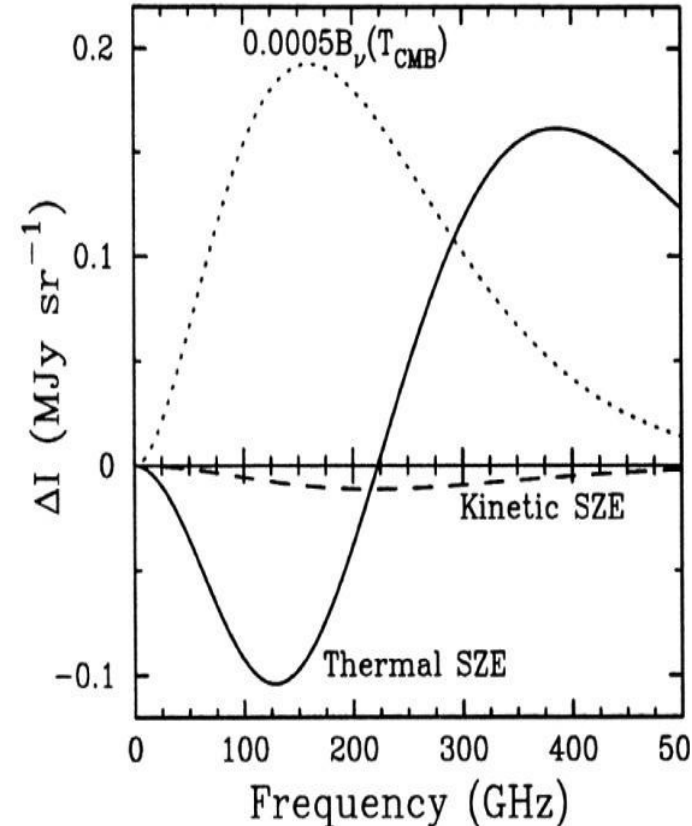
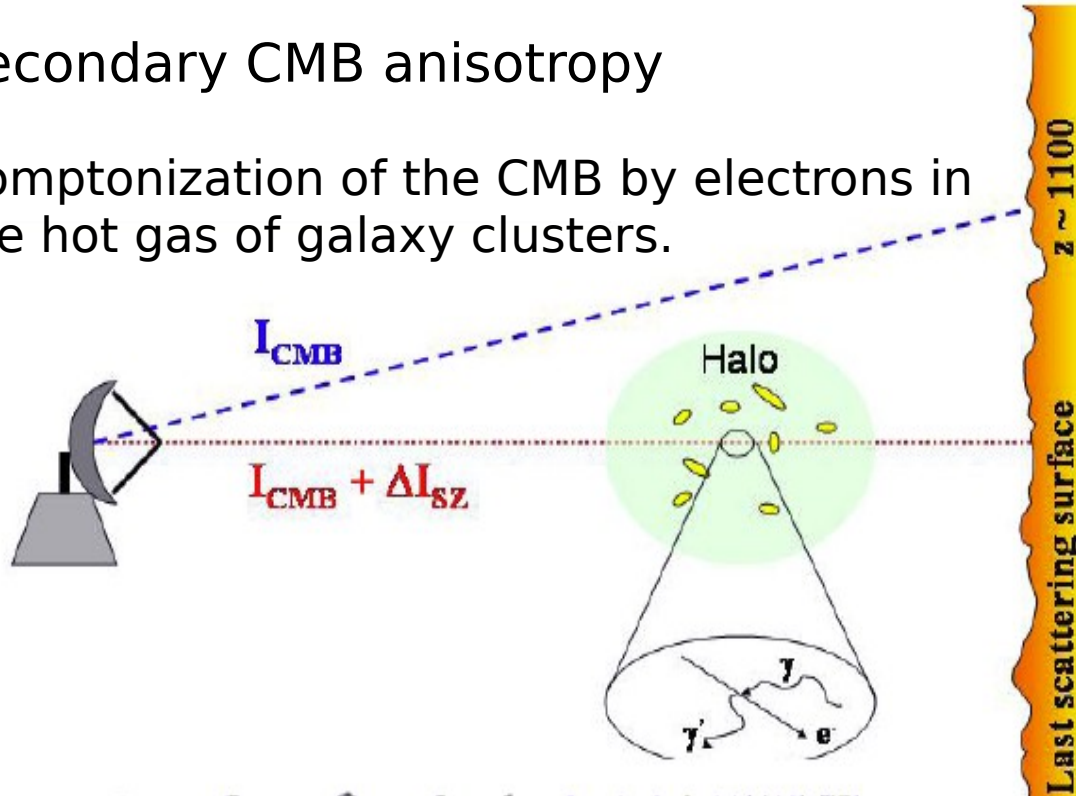
Outline

- CMB
- SZE
- $T_{\text{CMB}}(z)$
- Cluster parameter recovery with Planck HFI:
forecasts for H_0 and $T_{\text{CMB}}(z)$

The Sunyaev Zel'dovich Effect (SZE) (I)

Secondary CMB anisotropy

Comptonization of the CMB by electrons in the hot gas of galaxy clusters.



(Carlstrom JE A&A , 40, 643,2002)

Spectral distortion of the CMB due to the SZE

$$\Delta I_{SZ} = TSZ + KSZ + SZ_{CORREL}$$

Random motions of the scattering electrons

Systematic motions of the scattering electrons (Doppler effect)

The Comptonization parameter

$$\Delta I = I_0 h(x) \sigma_T \int n_e dl [\theta f(x) - \beta + R(x, \theta, \beta)]$$

$$x = h\nu/kT$$

$$\theta = kT_e/mc^2$$

$$\beta = v/c$$

R function= relativistic corrections

(Rephaeli 1995-Itoh et al. ApJ **502**, 7, 1998 - Shimon & Rephaeli ApJ **575**, 12, 2002)

$$\Delta I_{TSZ} = g(x) I_0 y$$

$$\Delta I_{KSZ} = -\beta h(x) I_0 \tau$$

$$y = \int \frac{kT_e}{m_e c^2} \sigma_T n_e dl = \frac{kT_e}{m_e c^2} \tau = y_0 f(\theta)$$

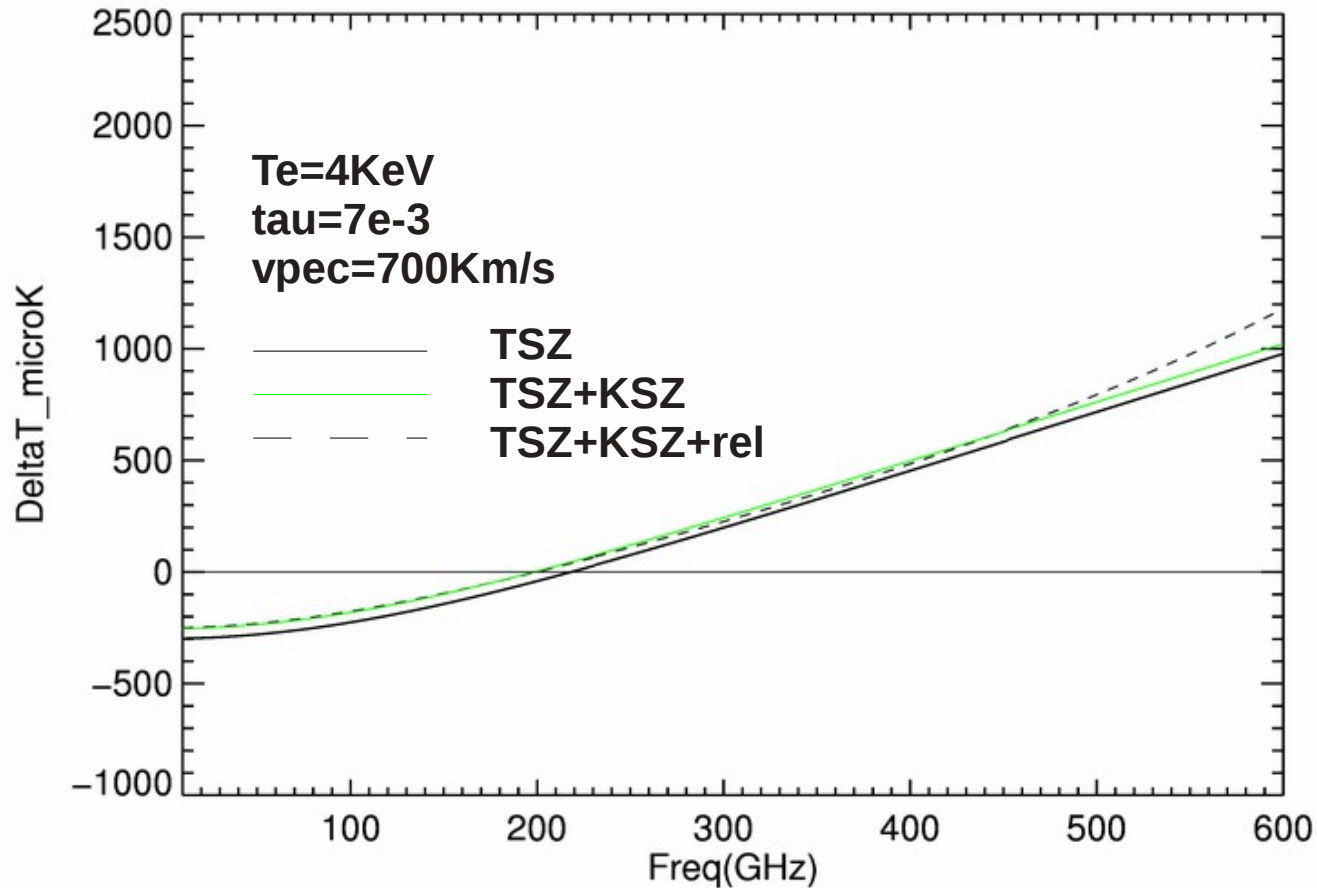
$$Y = \int y d\Omega$$

Ω = solid angle occupied by the source in the sky

$$\Delta T_{TSZ} = f(x) y T_{CMB}$$

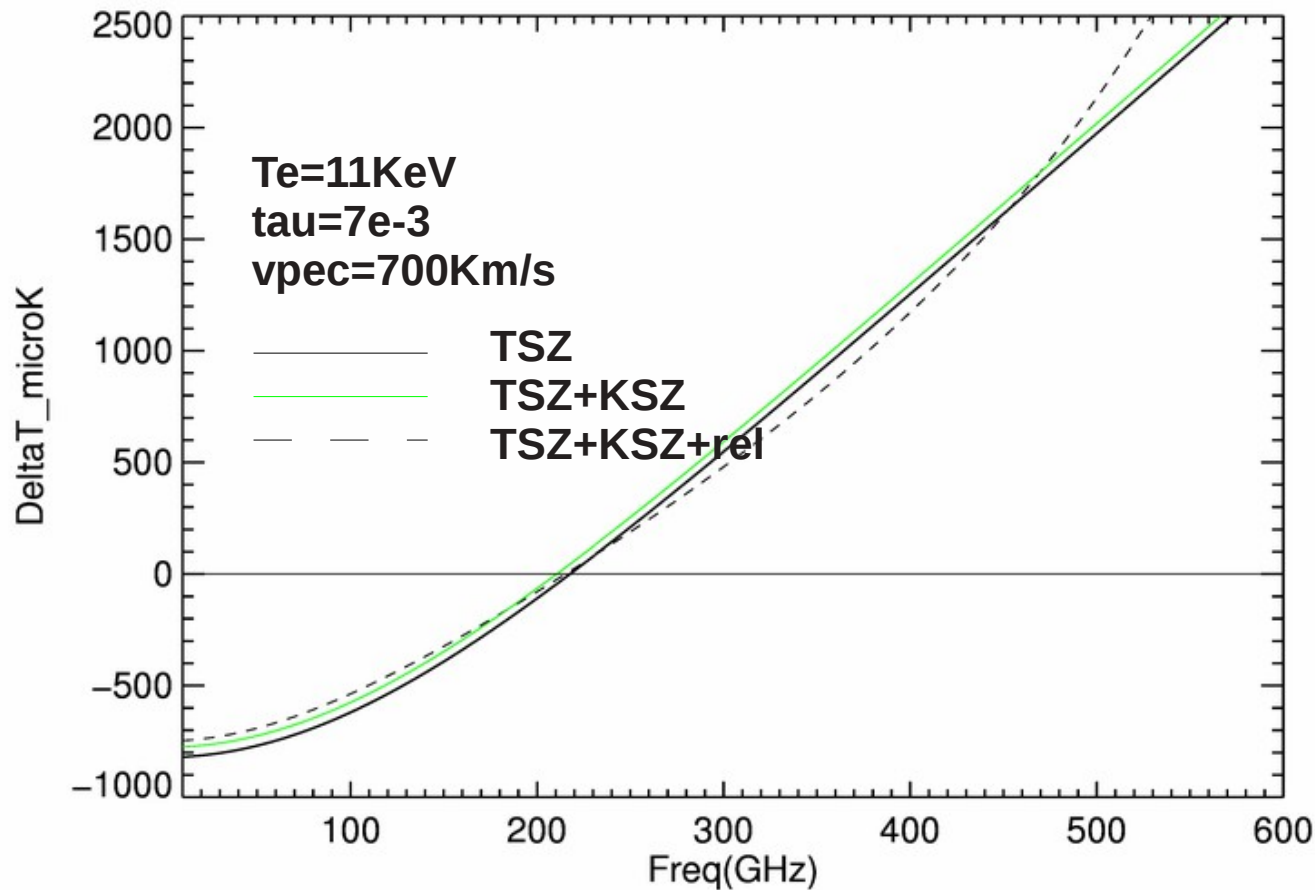
$$\Delta T_{KSZ} = -\beta \tau T_{CMB}$$

SZE in thermodynamic temperature (I)



In the non-relativistic regime the Kinematic SZ distortion is indistinguishable from a CMB temperature fluctuation.

SZE in thermodynamic temperature (II)



For massive clusters with $T_e \sim 10\text{KeV}$ the relativistic corrections to the SZE can be substantial near the null of the thermal effect (at high frequencies are order of few percent of the TSZ).

Relativistic corrections essential in determining H_0 (Battistelli et al 2003), v_{pec}

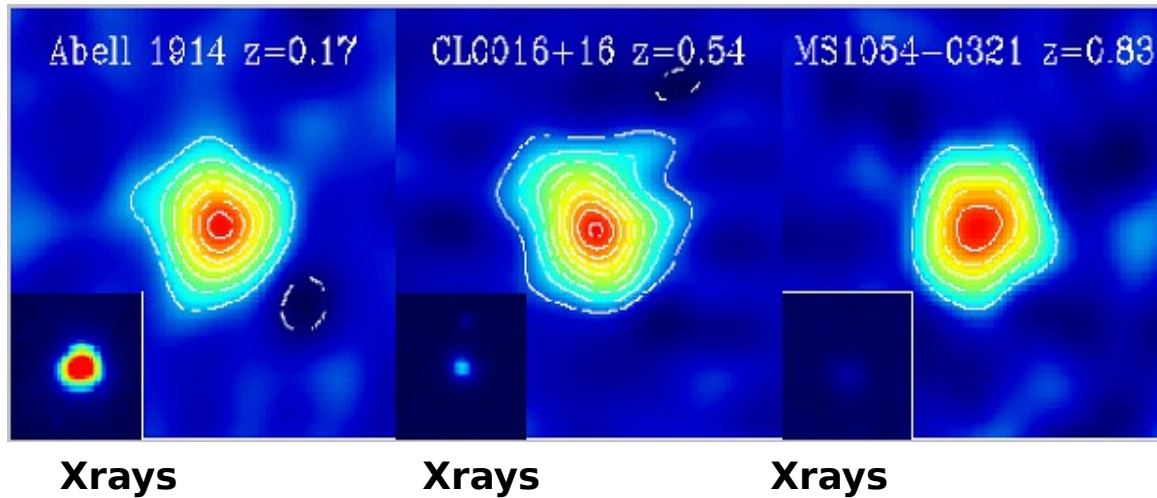
(Rephaeli 1995) and $T_{\text{CMB}}(z)$ (Battistelli et al 2002).

The Sunyaev Zel'dovich Effect (SZE) (II)

- Properties:
- unique spectral shape
 - Redshift independent
 - \propto electron pressure in cluster atmospheres

$$\Delta I_{SZ} \propto \int n_e dl$$

$$S_X \propto \int n_e^2 dl$$



Galaxy clusters

Physics:

- τ optical depth
- T_e electronic temperature
- v_{pec} peculiar velocity

Cosmology:

- $T_{CMB}(z)$
- H_0
- Ω_B
- evolution of abundance of clusters

Outline

- CMB
- SZE
- $T_{\text{CMB}}(z)$
- Cluster parameter recovery with Planck HFI: forecasts for H_0 and $T_{\text{CMB}}(z)$

$T_{\text{CMB}}(z)$: why measure it?

• **Observational test of the standard model:** $T_{\text{CMB}}(z) = T_0(1+z)$

$T_0 = (2.725 \pm 0.002)\text{K}$ solar system value measured by COBE/FIRAS (Mather et al. 1999)

• **Test of the nature of redshift (test of the Tolman's law)**

(Tolman. R. C., 1930, Proc. Nat. Acad, Sci., 16, 511) ; Sandage 1988; Lubin & Sandage 2001)

• **Constraints on alternative cosmological models**

(which rely on the physics of the matter and radiation content of the Universe):

- Λ -decaying models

(Overduin and Cooperstock, Phys.Rev.D, 58 (1998)); (Lima et al., MNRAS, 312 (2000); (Puy, A&A, 2004);

(Jetzer et al., 2010))

- Decaying scalar field cosmologies

- Cosmic opacity (Avgoustidis et al 2010)

• **Constraints on the variation of fundamental constants over cosmological time:**

test with search for non-standard effects that must be present if constants do vary (C.J.A.P. Martins 2010)

Dynamical Dark Energy: since a scalar field yielding dark energy also yields varying couplings, they can be used to reconstruct $w(z)$.

$T_{\text{CMB}}(z)$: first measurements

Measurements of CMB temperature traditionally through the study of excitation temperatures in high redshift molecular clouds.

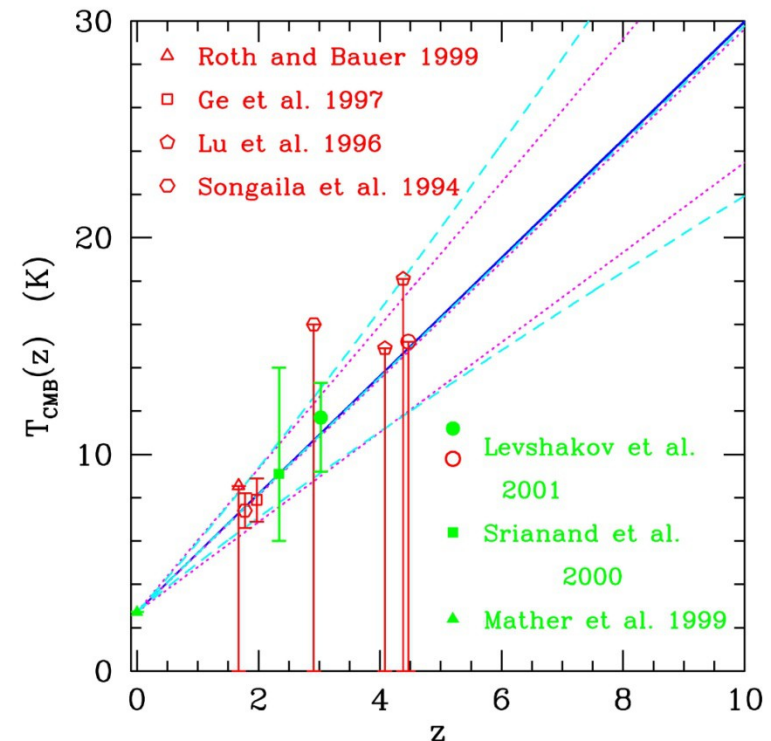
First attempt pioneered by (Bahcall and Wolf, 1968)

Many high redshift estimates of T_{CMB} at redshift of absorbers

(Songaila et al 1994; Lu et al. 1996; Ge et al 1997; Roth and Bauer, 1999; Srianand et al 2000; loSecco et al. 2001; Levshakov et al. 2002; Molaro et al. 2002; Cui et al. 2005)

Systematics:

- CMB is not the only radiation field populating the energy levels, from which transitions occur.
- detailed knowledge of the physical conditions in the absorbing clouds is necessary (Combes and Wiklind, 1999; Combes, 2007)



(LoSecco et al. Phys. Rev. D, 64, 123, 2002)

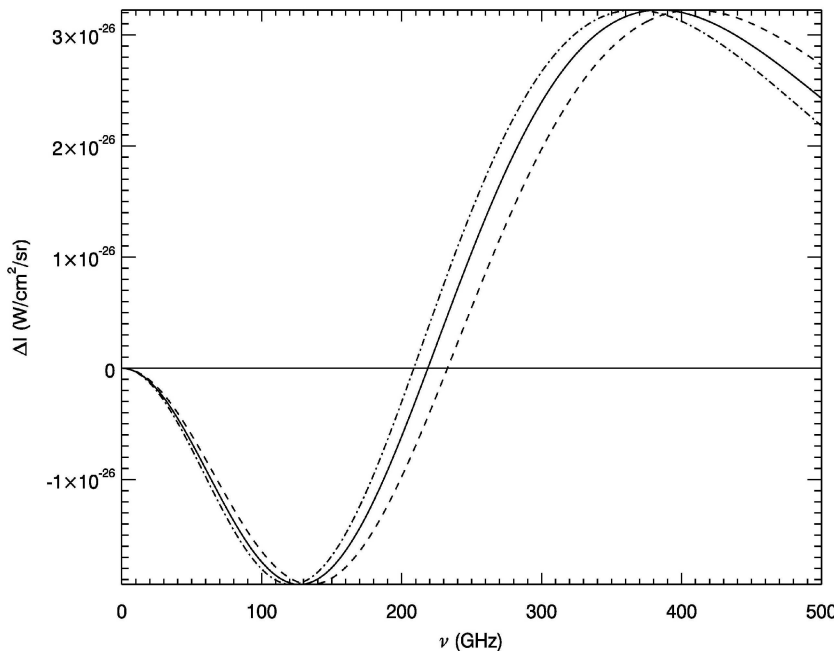
$T_{\text{CMB}}(z)$ from SZE (I)

(Fabbri R., F. Melchiorri & V. Natale. Ap&SS 59, 223, 1978; Rephaeli Y. Ap.J. 241, 858, 1980)

ΔI_{SZ} depends on frequency ν through the nondimensional ratio $h\nu/kT$:

$$x = \frac{h\nu(z)}{kT_{\text{CMB}}(z)} = \frac{h\nu_0(1+z)}{kT_0(1+z)} = \frac{h\nu_0}{kT_0}$$

redshift-invariant only for
standard scaling of $T(z)$



In all other non standard scenarios, the “almost” universal (remember rel. corrections!) dependence of thermal SZ on frequency becomes z -dependent, resulting in a small dilation/contraction of the SZ spectrum on the frequency axis.

Ex: $T_{\text{CMB}}(z) = T_{\text{CMB}}(0)(1+z)^{1-a}$

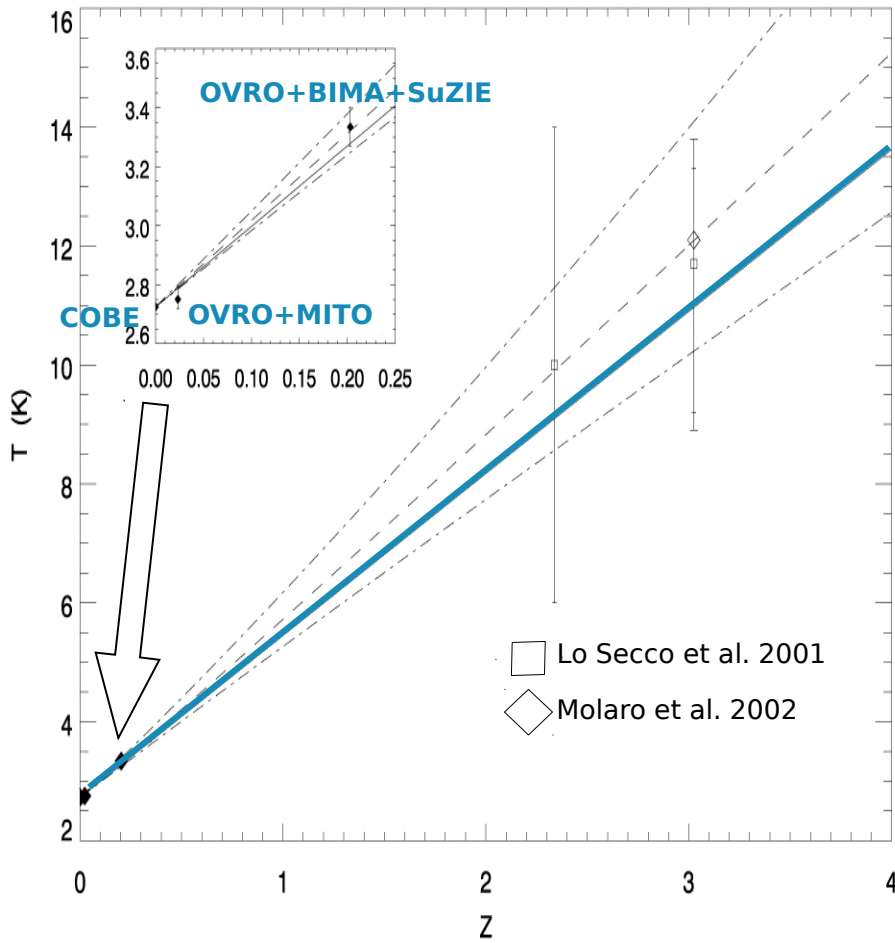
(Lima et al. 2000)

$$x' = \frac{h\nu_0(1+z)}{kT_0(1+z)^{(1-a)}} = \frac{h\nu_0}{kT_{\text{CMB}}^*}$$

where $T_{\text{CMB}}^* = T_{\text{CMB}}(0)(1+z)^{-a}$

$T_{\text{CMB}}(z)$ from SZE: first results

COMA+A2163



(Battistelli et al., ApJL 580, 101, 2002)

$$T_{\text{CMB}}(z=0) = 2.725^{+0.02}_{-0.02} \text{ K}$$

$$T_{\text{A1656}}(z=0.0231) = 2.789^{+0.080}_{-0.065} \text{ K}$$

$$T_{\text{A2163}}(z=0.203) = 3.377^{+0.101}_{-0.102} \text{ K}$$

$$T(z) = T_0(1+z)$$

$$T(z) = T_0(1+z)^{1-a}$$

$$T(z) = T_0[1+(1+\gamma)z]$$

$$a = -0.16^{+0.34}_{-0.32} \text{ (95\%c.l.)}$$

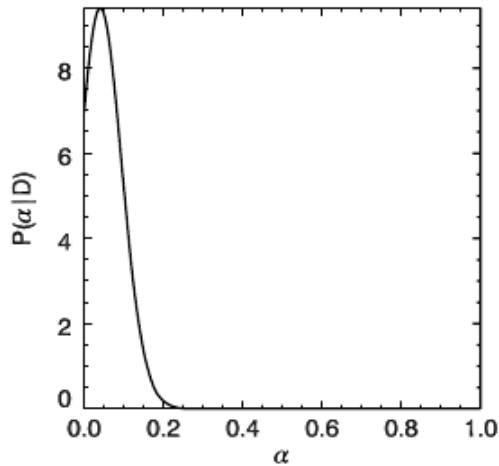
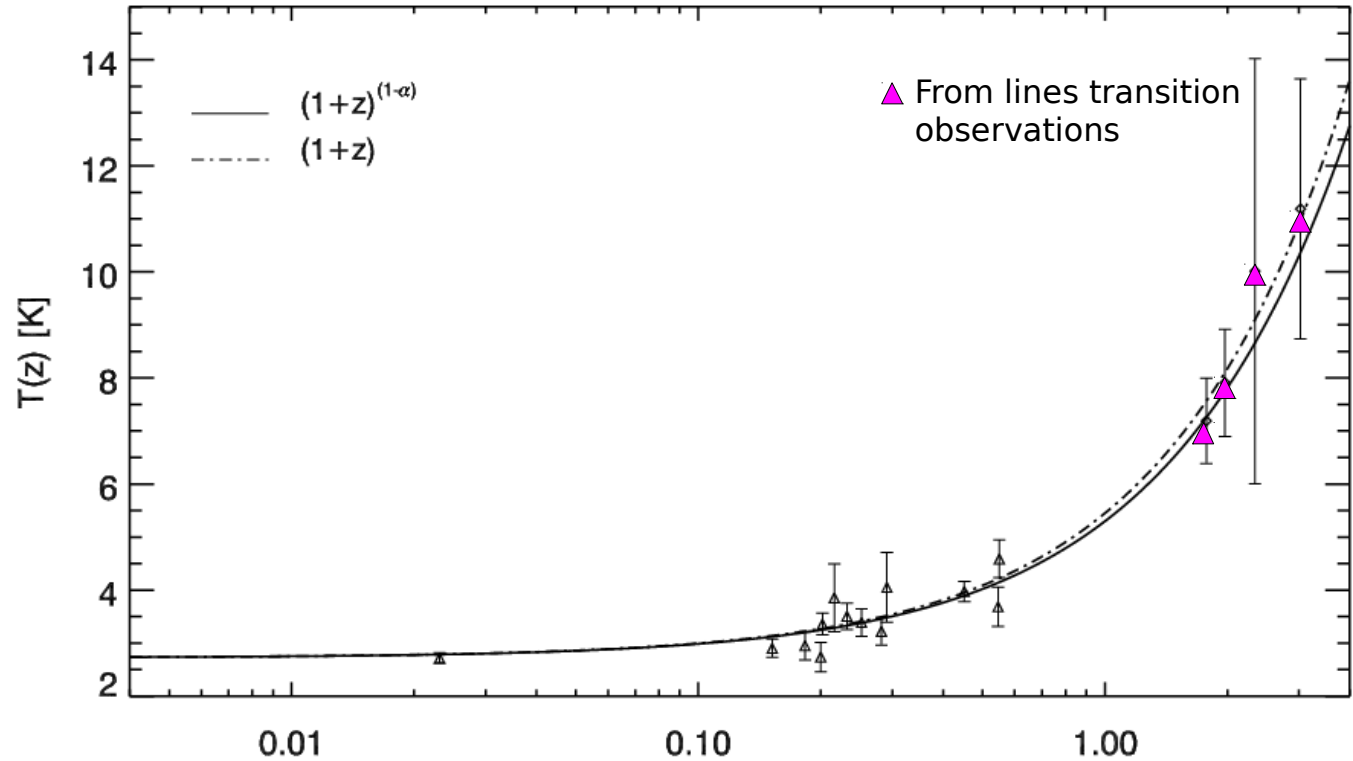
$$d = -0.17 \pm 0.36 \text{ (95\%c.l.)}$$

**Molecular microwave
transitions
CONSISTENT**

**Standard Model
CONSISTENT**

$T_{\text{CMB}}(z)$ from SZE: Results

Cluster	$T(z)$ (K)
A1656	2.72 ± 0.10
A2204	2.90 ± 0.17
A1689	2.95 ± 0.27
A520	2.74 ± 0.28
a2163	3.36 ± 0.20
A773	3.85 ± 0.64
A2390	3.51 ± 0.25
a1835	3.39 ± 0.26
A697	3.22 ± 0.26
ZW3146	4.05 ± 0.66
RXJ1347	3.97 ± 0.19
CL0016+16	3.69 ± 0.37
MS0451	4.59 ± 0.36



(Luzzi et al., ApJ 705, 1122, 2009)

Flat prior $\alpha \in [0,1]$ (theoretical motivation)
(Lima et al 2000)

All limits are at 68% probability level

RI $\alpha \leq 0.092$

DI (JL) $\alpha \leq 0.059$

DI (SL-MCMC) $\alpha \leq 0.12$ (including lines $\alpha \leq 0.079$)

$T_{\text{CMB}}(z)$ from SZ+ atom. Carbon. + CO

P. Noterdaeme et al.: The evolution of the Cosmic Microwave Background Temperature

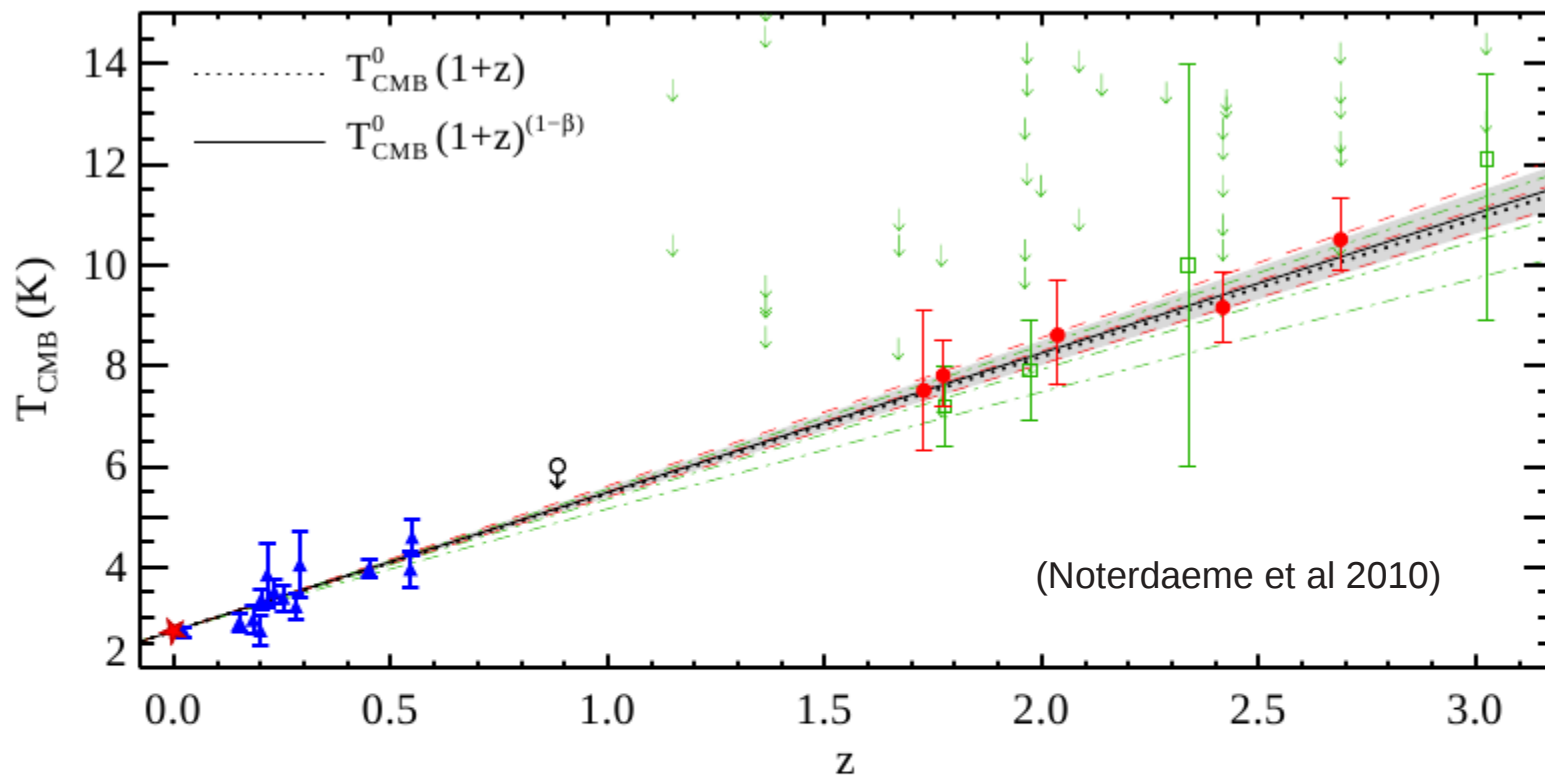


Fig. 4. The black-body temperature of the Cosmic Microwave Background radiation as a function of redshift. The star represents the measurement at $z = 0$ (Mather et al. 1999). Our measurements based on the rotational excitation of CO molecules are represented by red filled circles at $1.7 < z < 2.7$. Other measurements at $z > 0$ are based (i) on the S-Z effect (blue triangles at $z < 0.6$, Luzzi et al. 2009) and (ii) on the analysis of the fine structure of atomic carbon (green open squares: $z = 1.8$, Cui et al. 2005; $z = 2.0$, Ge et al. 1997; $z = 2.3$, Srianand et al. 2000; $z = 3.0$, Molaro et al. 2002). Upper-limits come from the analysis of atomic carbon (from the literature and our UVES sample, see Srianand et al. 2008) and from the analysis of molecular absorption lines in the lensing galaxy of PKS 1830-211 (open circle at $z = 0.9$, Wiklind & Combes, 1996). The dotted line represents the adiabatic evolution of T_{CMB} as expected in standard hot Big-Bang models. The solid line with shadowed errors is the fit using all the data and the alternative scaling of $T_{\text{CMB}}(z)$ (Lima et al. 2000) yielding $\beta = -0.007 \pm 0.027$. The red dashed curve (resp. green dashed-dotted) represents the fit and errors using S-Z + CO measurements (resp. S-Z + atomic carbon).

$T_{\text{CMB}}(z)$ from SZE: simulations

Simulated observations of 50 well known clusters
mock dataset analyzed to recover
input parameters of the cluster

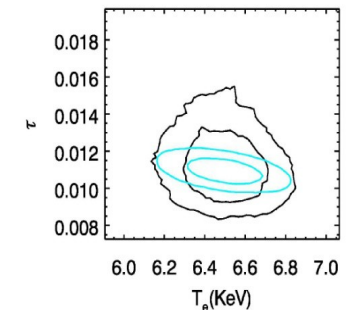
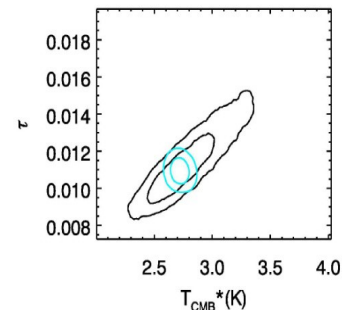
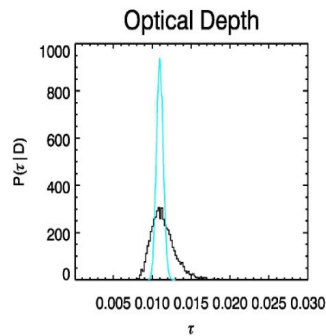
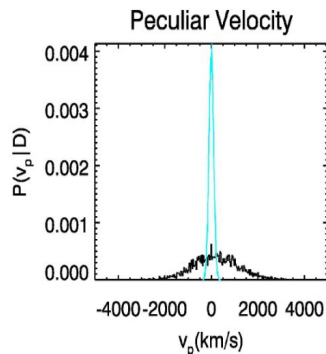
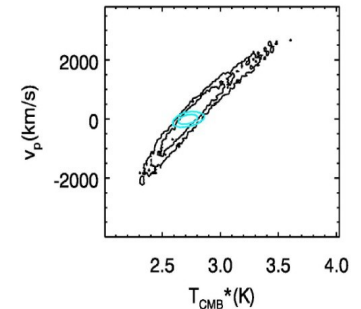
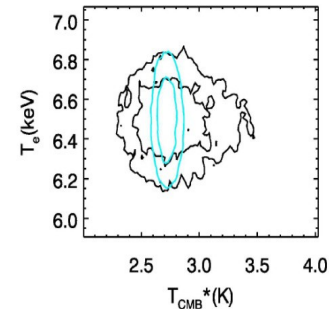
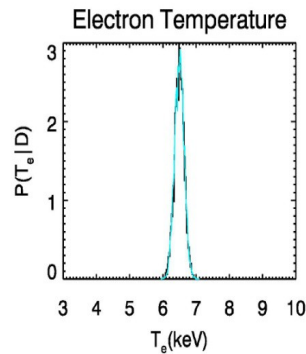
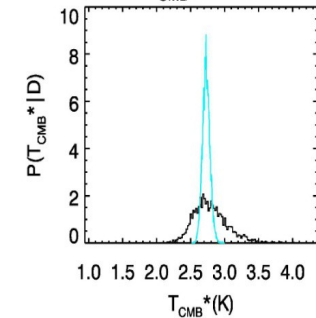
Analysis: MCMC

$$P(v_p) = N(0 \text{ km/s}, 1000 \text{ km/s}) \quad \text{—}$$

$$P(v_p) = N(0 \text{ km/s}, 100 \text{ km/s}) \quad \text{—}$$

$$P(T_e) = N(6.50 \text{ KeV}, 0.14 \text{ KeV})$$

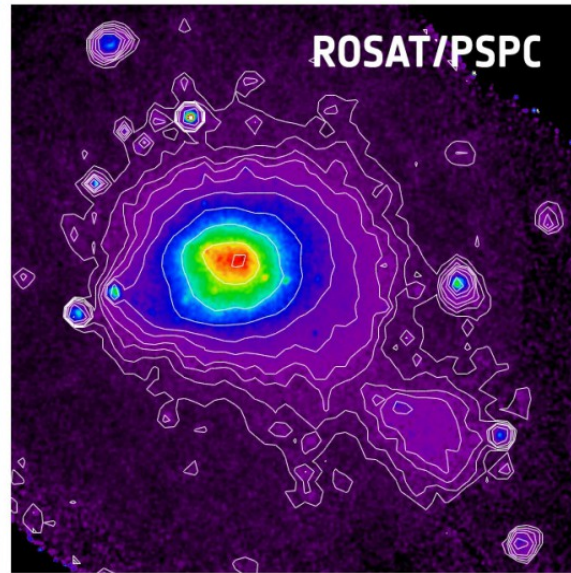
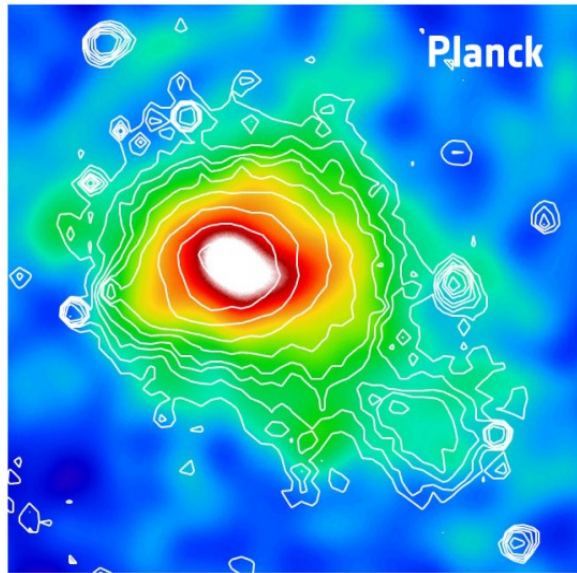
ABELL0085 : $T_{\text{CMB}}(z)/(1+z)$; $z = 0.0550$



Outline

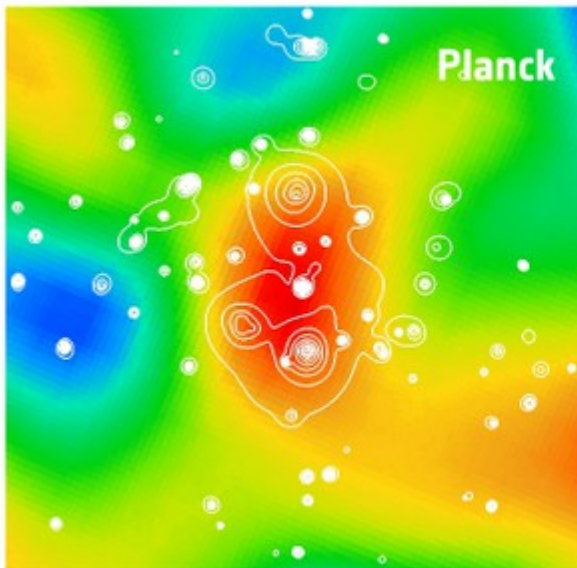
- CMB
- SZE
- $T_{\text{CMB}}(z)$
- Cluster parameter recovery with Planck HFI:
forecasts for H_0 and $T_{\text{CMB}}(z)$

SZE with Planck



COMA cluster

Image credit: ESA/HFI and LFI consortia; ESA/ROSAT



The first supercluster discovered through its SZE

Image credit: ESA/HFI and LFI consortia; ESA/XMM-Newton

Cosmological parameters from a survey of well known X-ray and optical clusters

Planck HFI ideal to study SZE in galaxy clusters

- **spectral coverage**: positive and negative part of the spectral distortion, ideal for cluster detection and to break cluster parameters degeneracy
- **angular resolution**: nearby clusters resolved and confusion reduced at large depth
- **full sky survey**: thousand of clusters

Survey dedicated to a sample of well known clusters in the X-ray and optic

subsample of the complete catalog

selection of the subsample:

- nearby clusters: H_0 (Hubble diagram- SZ-X method)
- medium redshift clusters: test of $T_{\text{CMB}}(z)$; optimal redshift range to test fine structure variation and Dark Energy
- high redshift clusters: feasibility test to extract Ω_M from the Hubble diagram

Catalogue (I)

- 166 clusters using X-Rays Clusters Databased (BAX)

Cluster name	
RA (J2000)	
DEC (J2000)	
z	Redshift
F_x	X flux in the ROSAT band (0.1-2.4 KeV) (10-12 erg/s/cm ²)
Reference F_x	
L_x	X Luminosity in the ROSAT band (0.1-2.4 KeV) (10 ⁴⁴ erg/s)
Reference $-L_x$	
Bande -Inf (KeV)	
Bande-Sup(KeV)	
T_x	X-ray Gas temperature (KeV)
σ_{Tx}	
Reference T_x	
Instrument	
Rcore	Core radius (arcsec)
σ_{Rcore}	
Reference- R_{core}	
β	Slope of the gas density profile (isothermal beta model)
σ_β	

Catalogue (II)

Derived parameters

n_{e0}	Central electronic density (isothermal beta model+ Furuzawa et al., 1998)
y_{th}	Central comptonization parameter
τ_{th}	Optical depth
Y_{int}	Comptonization parameter integrated over the cluster extent
DA_{SZX}	Angular distance

Simulation

Planck HFI instrumental characteristics (Bluebook 2005) :

- Frequency bands: 100, 143, 217, 353 GHz
(545, 857 GHz not included: ideal for removing foregrounds)
- CMB and foregrounds assumed previously removed
- NET: 50, 62, 91, 277 $\mu\text{K}\sqrt{\text{s}}$
- Number of detectors: 8,12,12,12
- Angular resolution: 9.5, 7.1, 5.0, 5.0 arcmin
- Integration time: 10 s/cluster (uniform sky coverage and 2 years of observation)
- Integration time multiplied for the number of detectors
- Error estimates on the SZ signal take into account beam dilution

Forecasts for SZ signal assume Isothermal beta model

Data analysis

- Mock dataset analyzed to recover the original input cluster parameters.
- MCMC algorithm: allows to explore the full space of the cluster parameters (τ , v_p , T_e) + T_{CMB} (including calibration uncertainty: scale factor).
- MCMC: generates random sequences of parameters, which simulate posterior distributions for all parameters (Lewis and Bridle 2002)
- Metropolis & Hastings approach
- Gelman & Rubin test for convergence and mixing of chains

Priors: $P(T_{ei}) = N(E(T_{ei}), \sigma(T_{ei}))$ X-ray data

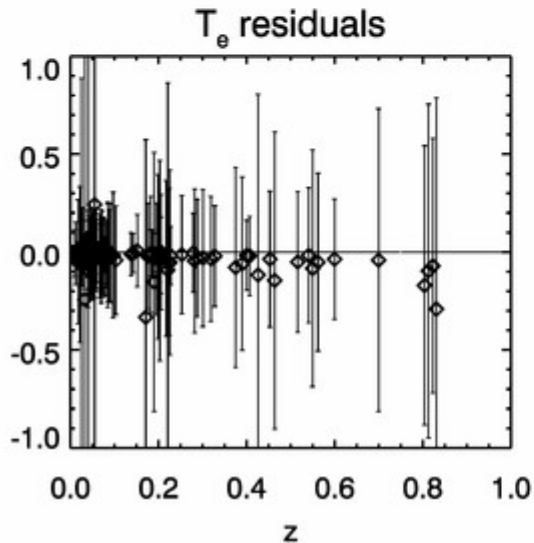
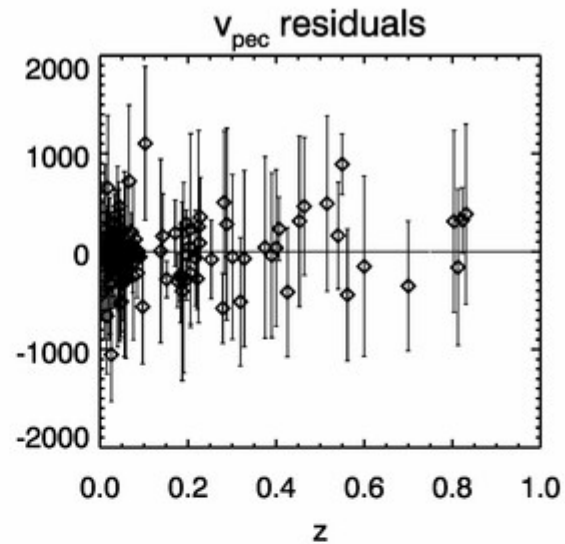
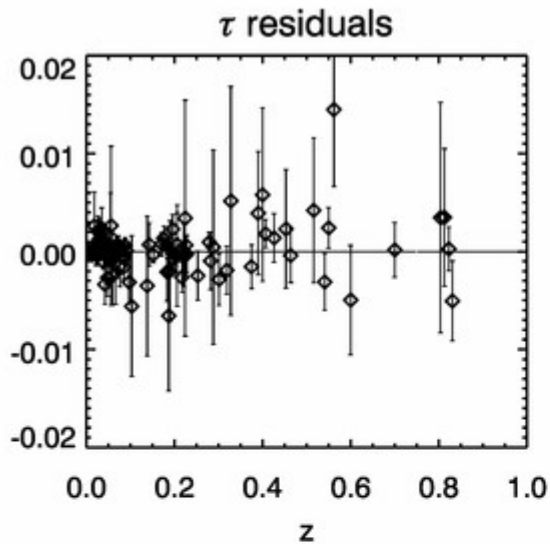
$$P(v_p) = N(0 \text{ km/s}, 1000 \text{ km/s})$$

$$P(\tau) = \text{flat (con } \tau \in [0, 6\tau_{th}]); N(\tau_{th}, 2\tau_{th})$$

$$P(C) = N(1, 0.01); N(1, 0.001)$$

$$P(T_{\text{CMB}}) = \text{flat; fixed to } T_0^*(1+z)$$

TSZ+KSZ+rel (I)

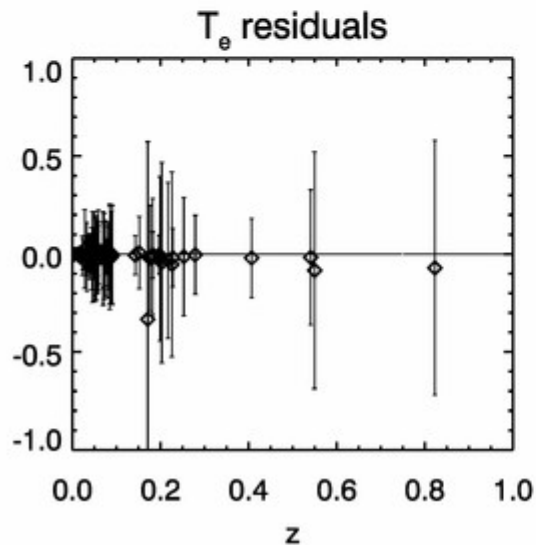
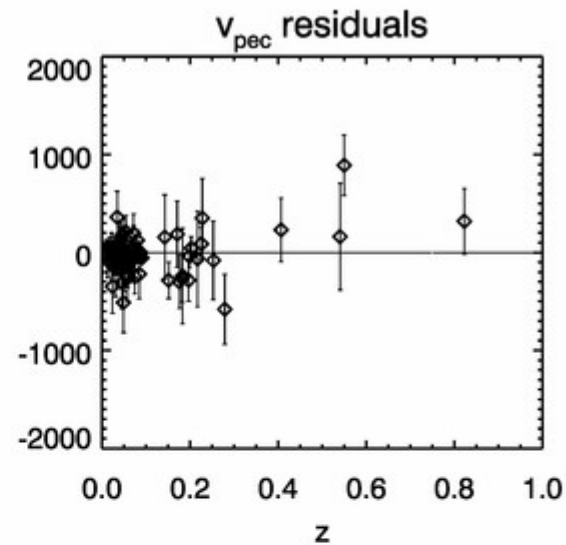
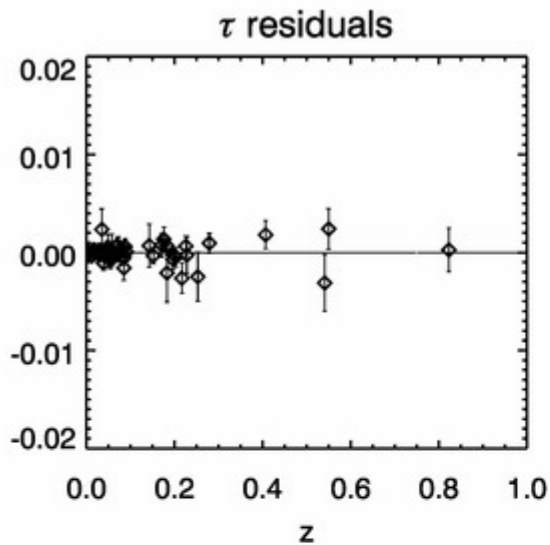


Initial NCLs = 166 (T_{CMB} fixed)

Excluded Cls with flat $P(\tau|D)$:

Final NCLs = 129

TSZ+KSZ+rel (II)



Initial NCLs = 166

Excluded Cls with flat $P(\tau|D)$
and with $\text{SNR}(\tau) \leq 6$:

Final NCLs = 71

Possible constraints on v_{pec} !

V_{pec} : why measure them?

- Test homogeneity on large scale by measuring peculiar velocities: they probe the mass distribution directly (Lahav 1999).
- The SZE offers a way to measure peculiar velocities with a redshift independent accuracy.
- Test theories of structure formation and evolution.
On scales probed by galaxy clusters, the underlying density fluctuations are largely in the linear regime and therefore very close to the initial conditions from which large scale structures developed (Aghanim et al 2001).

Method SZ-X to determine distances

Method SZ-X (Cavaliere et al, 1977)

Advantages of the technique:

- Completely independent of other techniques
 - Measures distances at high z directly, without any intervening chain of distance estimators (as in the usual distance ladder).
-
- Constraints complementary to those set by the number density of clusters in redshift space.
 - A sample of ~ 100 high redshift clusters: traces the expansion history of the Universe, valuable independent check respect to SNIa (Molnar et al. 2002)
 - SZ-X method is a physical method, based on relatively simple gravitational virialization of clusters, as opposed to complicated physics and chemistry involved in galaxy formation and supernovae explosion.

Data analysis

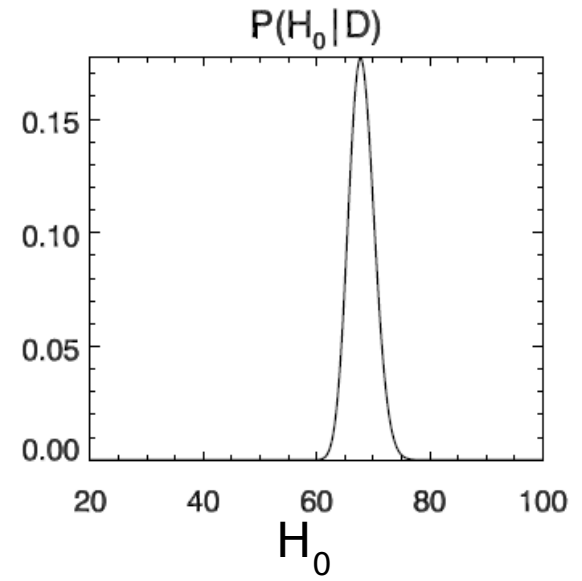
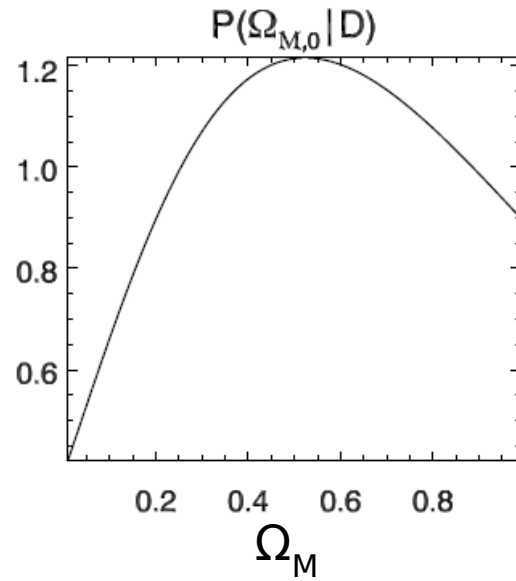
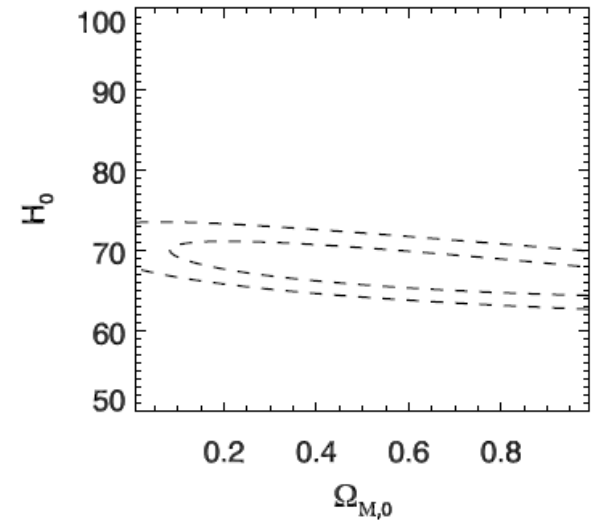
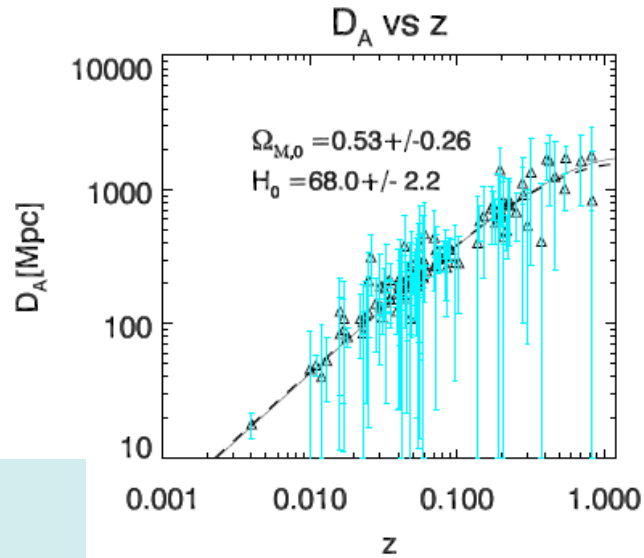
- Posteriors for all parameters
- Clusters with almost flat τ posterior excluded from the sample
- Recovered parameters are combined with X-ray fluxes to extract distances
- Sample (108 clusters) used to produce the Hubble diagram

Results (I)

$$E_X \propto \int n_e^2 dl$$

$$A_{SZ} \propto \int n_e dl$$

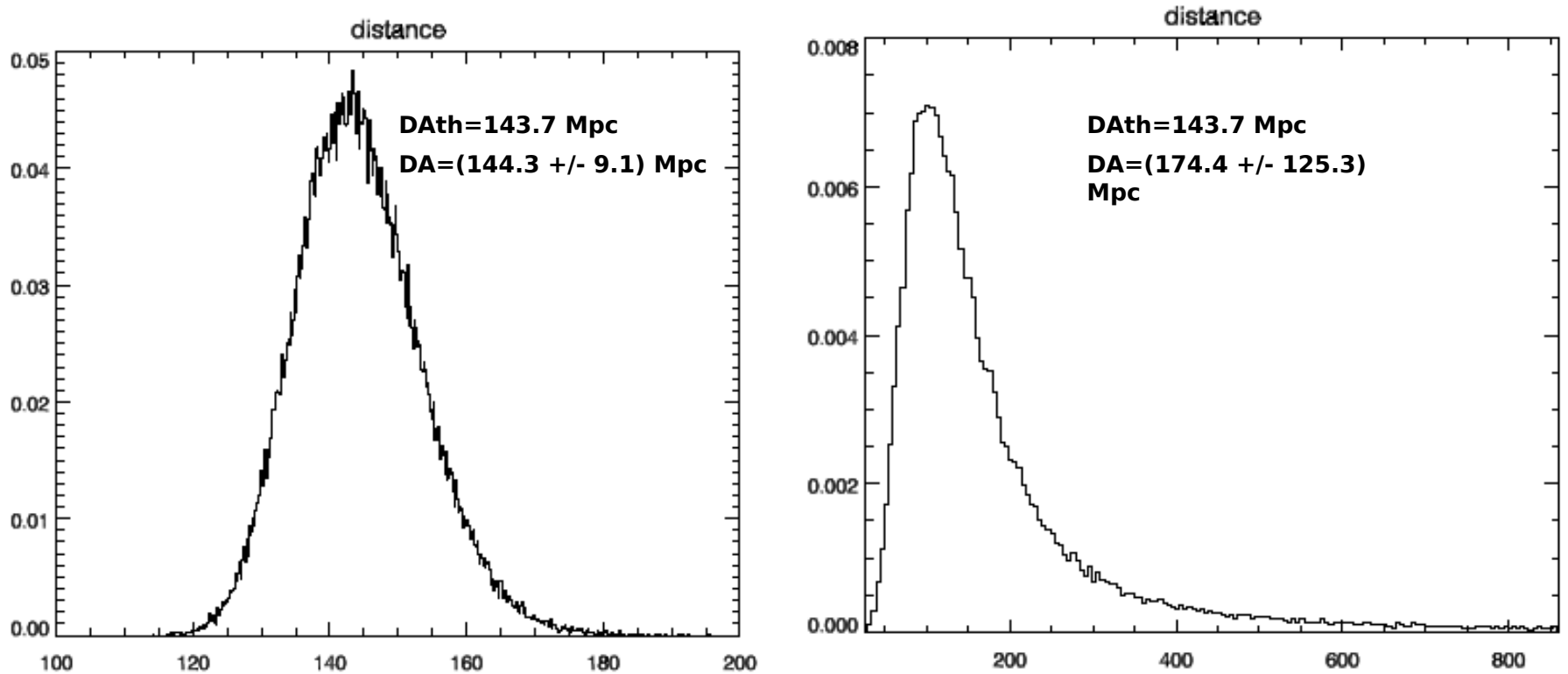
$$\frac{A_{SZ}^2}{E_X \theta} \longrightarrow D_A$$



Results (II)

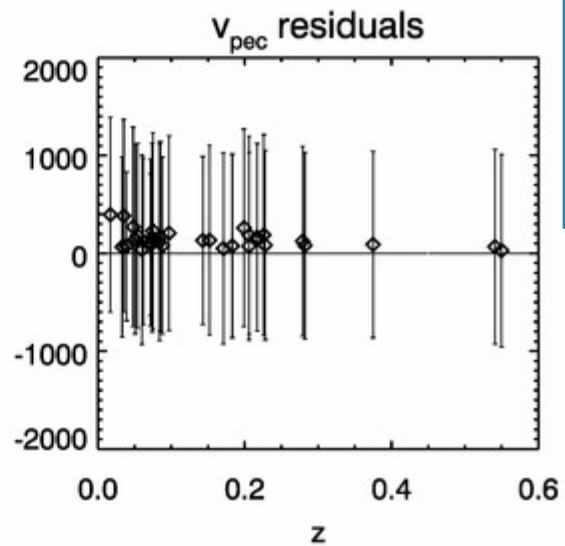
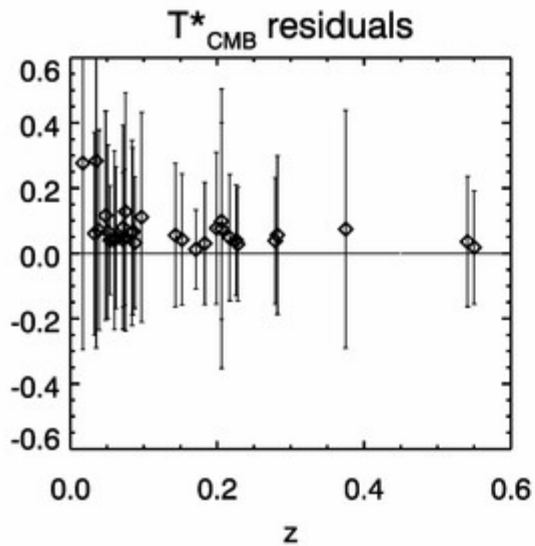
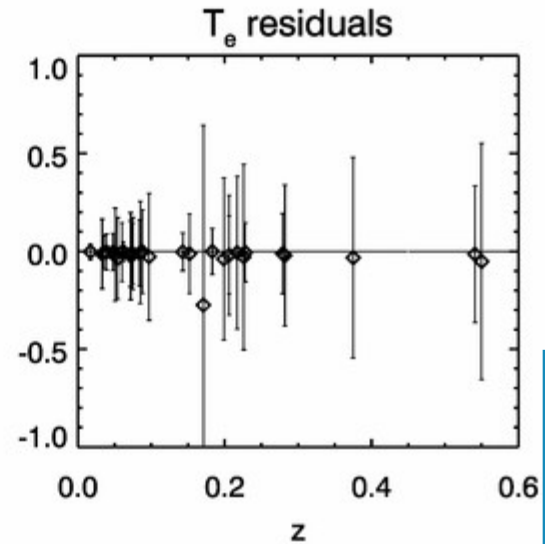
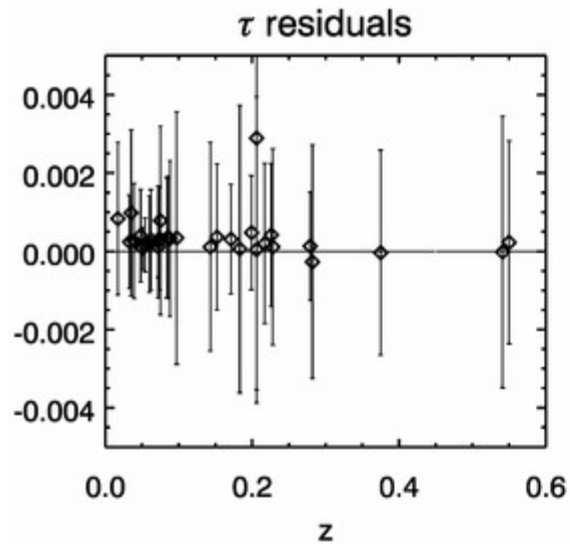
- Extraction of H_0 and Ω_M assuming Λ CDM:
priors: $P(H_0) = \text{flat } (H_0 \in [20,100] \text{ Km/s}),$
 $P(\Omega_M) = \text{flat } (\Omega_M \in [0;1])$
- 3% sensitivity on the Hubble constant
- Ω_M not constrained. Need for complementary constraints from other dataset and/or larger redshift exploration.

Bias in the determination of H_0



Angular distance for the cluster 2A0335+096. Left: histogram of angular distance as obtained by Montecarlo using the expression of Furuzawa et al. (1998) and assuming all parameters SZ and X-ray known with errors at 1%. Right: as above but with all parameters known with gaussian distribution and errors at 10%.

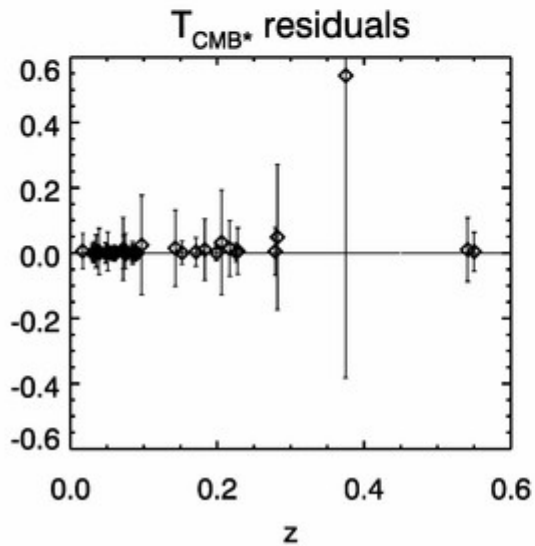
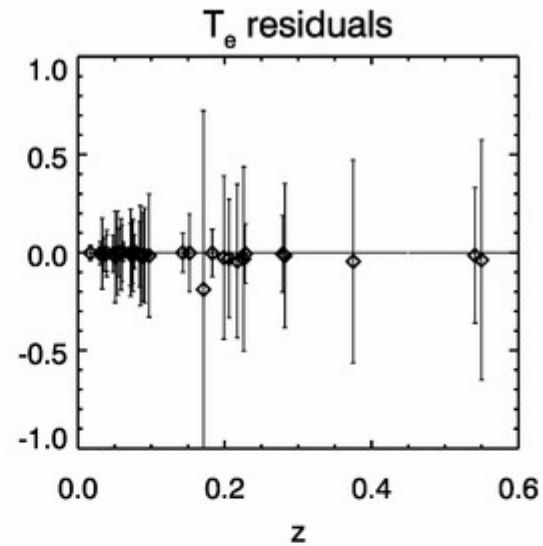
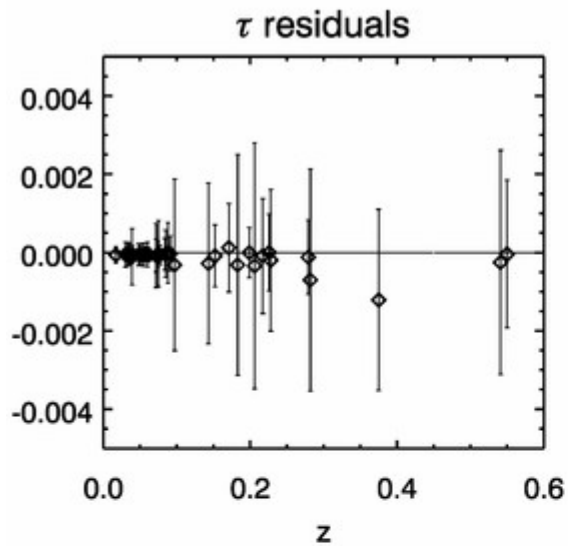
TSZ+KSZ+rel+T_{CMB}



Sample:
42 CL
(Planck cls \cap BAX
with Θ_c)

32 CL with
no flat $P(\tau|D)$

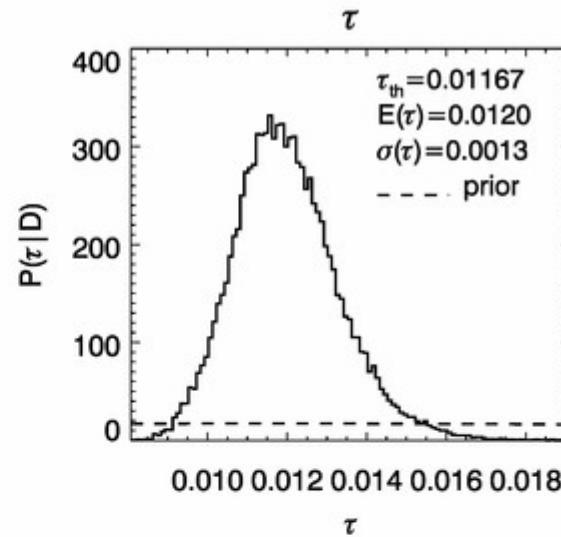
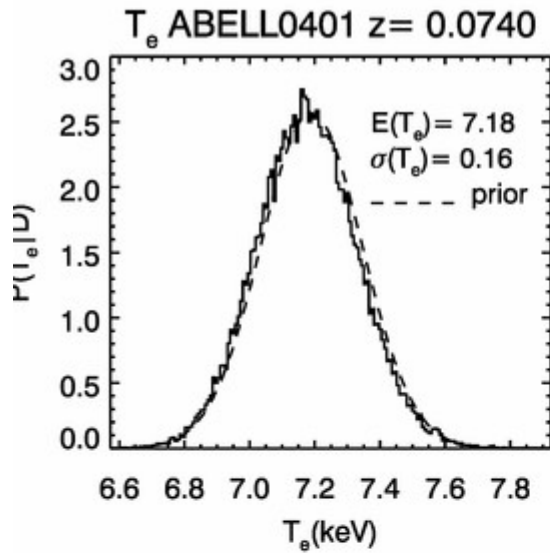
TSZ+rel_{TSZ}+T_{CMB}



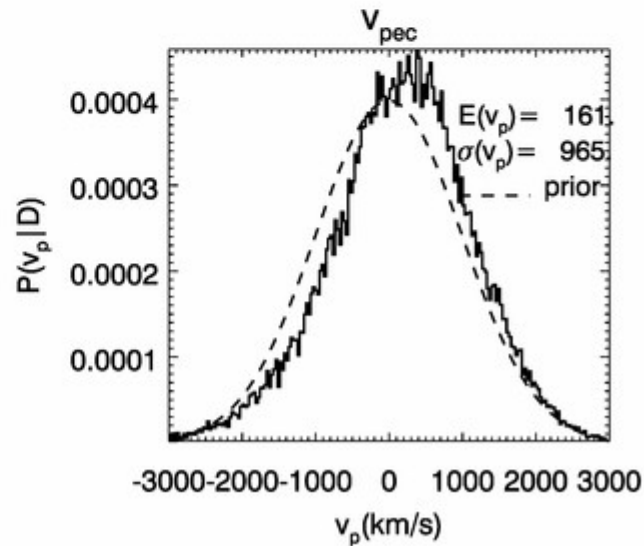
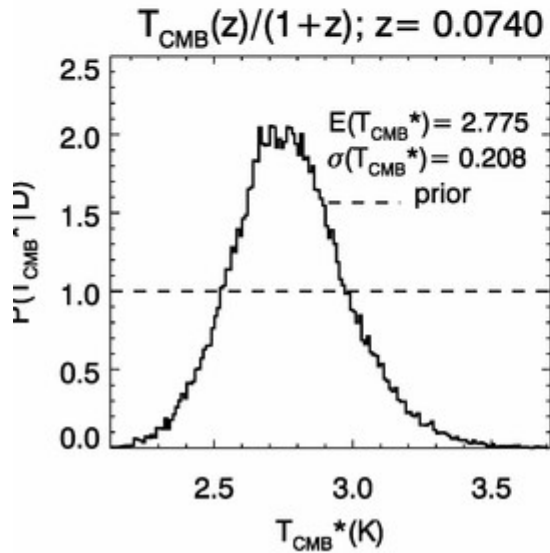
Sample:
42 CL
(Planck cls \cap BAX
with Θ_c)

37 CL with
no flat $P(\tau|D)$

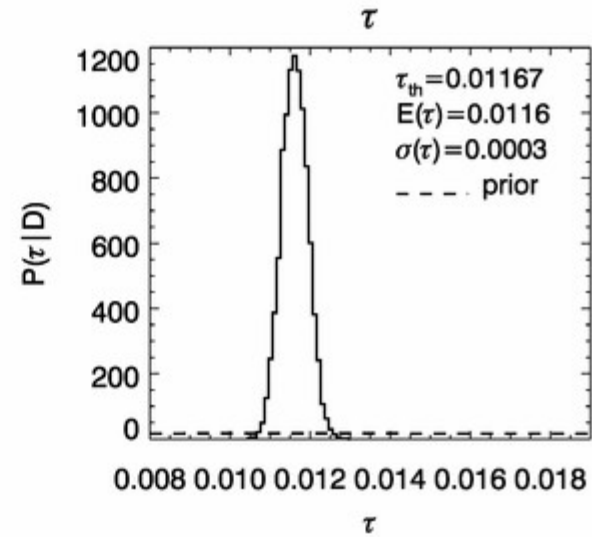
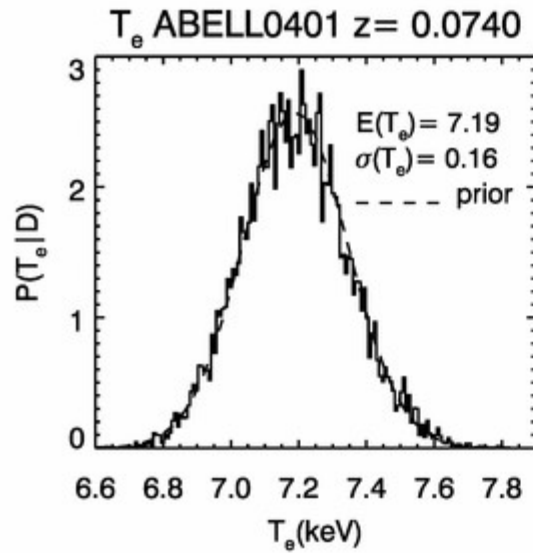
TSZ+KSZ+rel+T_{CMB}



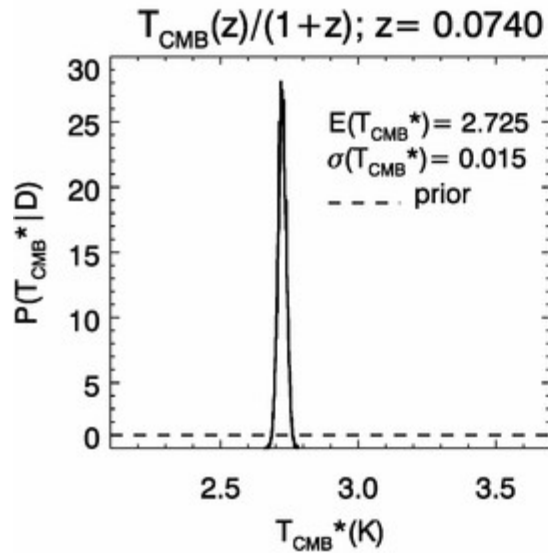
$\Theta_c = 2.37'$



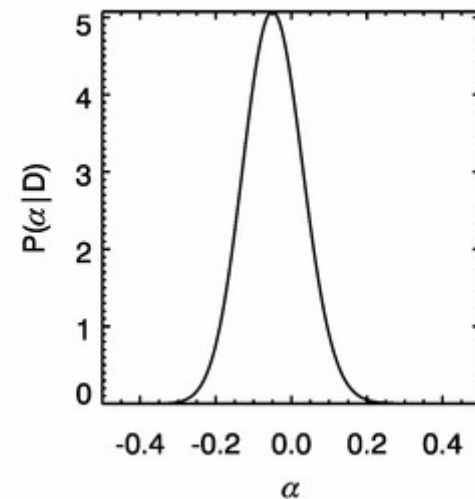
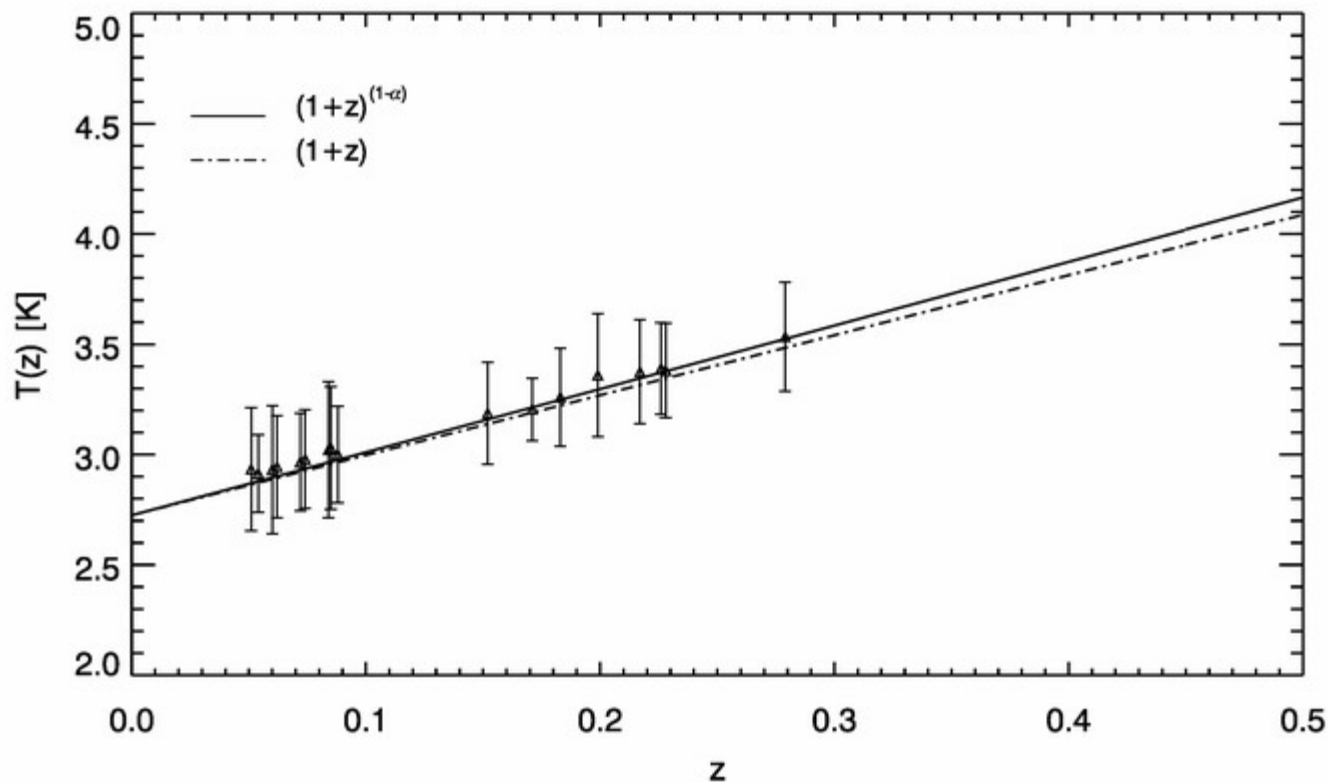
TSZ+rel_{TSZ}+T_{CMB}



$$\Theta_c = 2.37'$$



$T_{\text{CMB}}(z)$ (KSZ included)

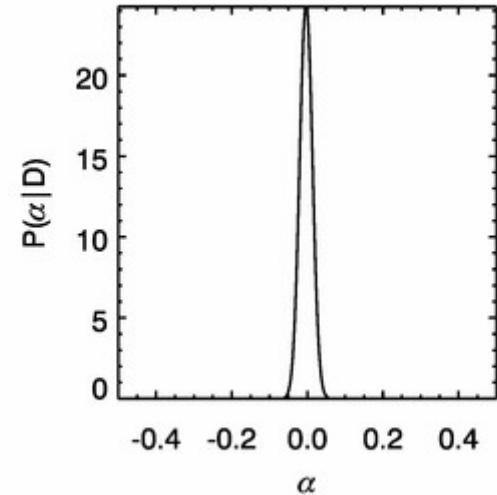
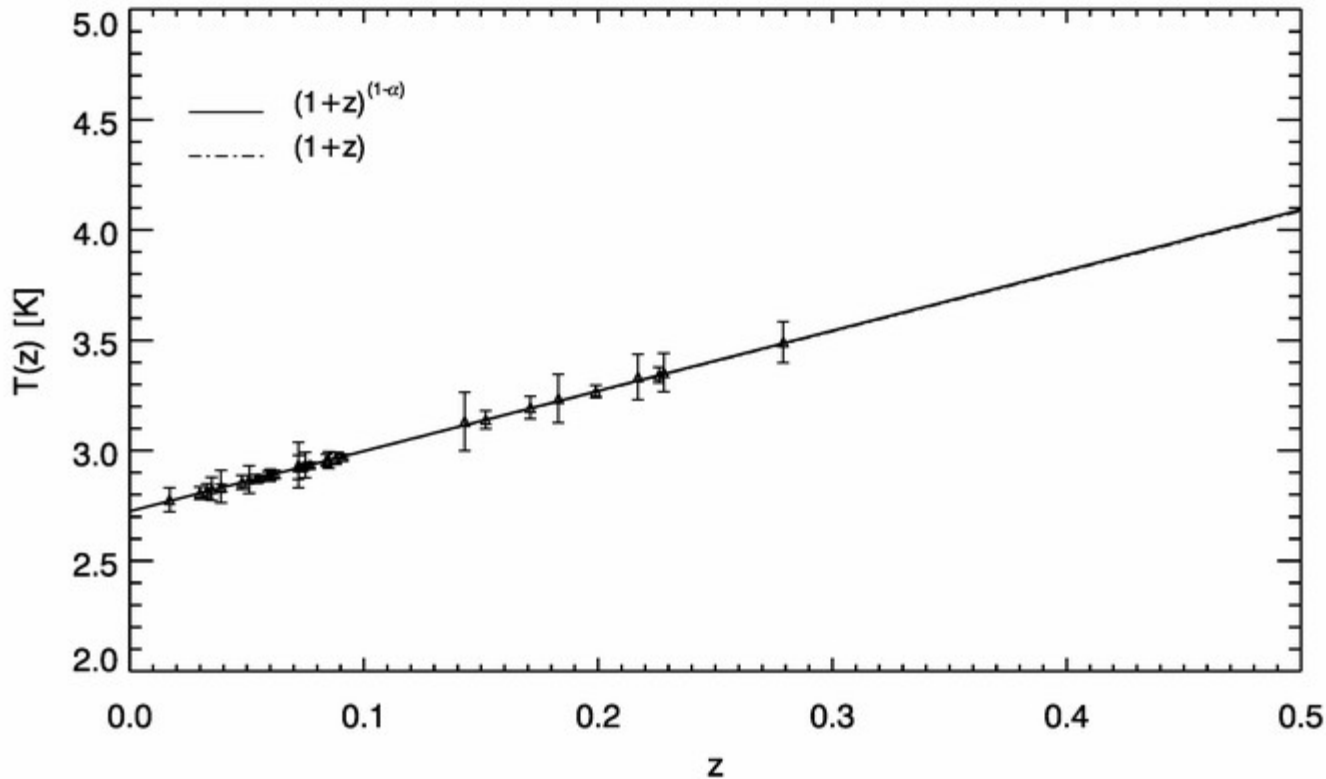


$$\alpha = -0.047 \pm 0.079$$

19 clusters selected with 2 conditions:

- Excluded all clusters with flat τ posterior
- $\text{SNR}(\tau) \geq 6$

$T_{\text{CMB}}(z)$ (no KSZ)



$$\alpha = -0.003 \pm 0.016$$

37 clusters selected with 2 conditions:

- Excluded all clusters with flat τ posterior
- $\text{SNR}(\tau) \geq 6$

Conclusions

- SZE is an original tool to observationally test the standard scaling of T_{CMB} and its isotropy up to the redshift of galaxy clusters and to put constraints on alternative cosmological models.
- With Planck HFI possible constraints on v_{pec} ($\sigma_{v_{\text{pec}}}$ order of few hundred of km/s) for Cls with $\text{SNR}(t)^{36}$.
- SZ-X technique for measuring distances: H_0 with a method completely independent of others (with Planck HFI 3% sensitivity on H_0).
- If Kinematic component removed altogether with CMB anisotropies component: with Planck up to 0.6% sensitivity on $T_{\text{CMB}}(z)$ (otherwise 7% sensitivity). With only tens of clusters better constraints on α with respect to present results with SZ+Atomic carbon+CO.